PAPER

Compound Scattering Matrix of Targets Aligned in the Range Direction

Kenji KITAYAMA[†*], Yoshio YAMAGUCHI[†], Jian YANG[††], *and* Hiroyoshi YAMADA[†], *Regular Members*

SUMMARY The Sinclair scattering matrix is defined in a fixed radar range. If a radar target extends in the range direction, the reflected signal or the compound scattering matrix will undergo interaction of multiple reflections. Since scattering matrix is subject to target parameters such as shape, size, orientation, material, and radar parameters as frequency, polarization, and incidence angle, it is difficult to specify a representative scattering matrix of a general target. Therefore we choose the simplest target, wire, and its scattering matrix to examine the effect of targets aligned in the range direction with respect to the compound scattering matrix. First, we present a simple formula for the compound scattering matrix of wires with the phase difference due to spacing. Then, we employed the FDTD method to examine the scattering phenomena, changing the spacing in the range direction. The FDTD result reveals that two wires can become sphere (plate) and dihedral corner reflector (diplane) component generators; and that four wires can become a good helix component generator. These phenomena are verified with a laboratory measurement. From the result, the target decomposition should be carefully carried out in terms of range. If a range resolution of a radar is not high enough, the scattering matrix of the desired target may be affected by the targets behind.

key words: *scattering matrix, FDTD, radar polarimetry*

1. Introduction

The Sinclair scattering matrix, which consists of polarimetric reflection coefficients of a radar target, is the most fundamental measurable quantity in polarimetric radar systems. It plays an important role in advanced polarimetric remote sensing, from which we can deduce scattering mechanism corresponding to single bounce, double bounce, and generation of circular polarization. This information leads to classification and identification of targets [1]–[3].

If a point target exists in a fixed range, the target scattering matrix acquired with a radar is uniquely defined. However, if several targets exist in the same range direction, there will be multiple scattering phenomena and the compound scattering matrix may not be defined uniquely.

If we are concerned with three length parameters on radar sensing, i.e., the radar range resolution ΔR, the wavelength λ, and the target spacing d, then how is the scattering matrix related to these parameters ? As shown in Fig. 1, the scattering matrix of target 1 can be represented by $[S]_1$ provided that $d >> \Delta R$. In this case, the scattering matrix is well defined. However, if $d < \Delta R$, the compound scattering matrix of the two targets will be quite different from $[S]_1 + [S]_2$. Since the radar has a range resolution $\Delta R = \frac{c}{2B}$ which is determined by the bandwidth B of the transmitted signal, the question is how to represent the compound scattering matrix of multi-point targets within the range resolution. This is the main topic of the paper.

So, we will examine the compound scattering matrix of point targets aligned in the range direction only. First, we briefly state some necessary theory on radar polarimetry in Sect. 2 which will be used in the following sections. Then we propose a simple formula of the compound scattering matrix of two targets which depends on the spacing with respect to the wavelength of the radar frequency. The point targets chosen in this paper are wires which are long enough compared to wavelength and have small radii. Since a wire target has physically simple structure and is easy to understand from the polarimetric point of view, we concentrate our attention on the properties of the compound scattering matrix of wires. In the following, the FDTD analysis [4], [5] is carried out for two and four wires. Using two wires with different distance, we obtain several special scattering matrices, which are usually corresponding to a sphere (plate) and a diplane (dihedral corner reflector), and with four wires we find out they can become a good circular polarization generator (helix). Features of these targets and

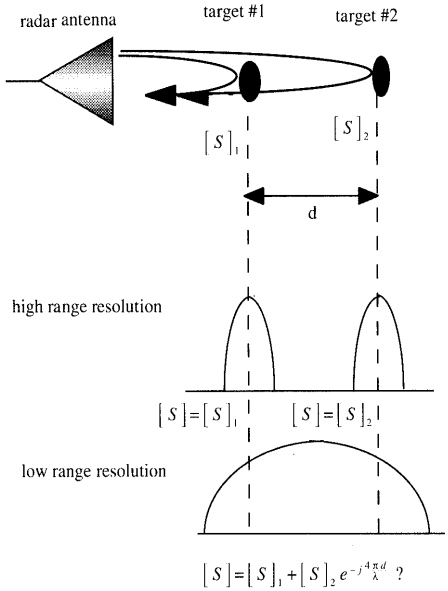

Fig. 1 Scattering matrix and range resolution.

Manuscript received January 28, 2000.
Manuscript revised July 10, 2000.

† The authors are with Niigata University, Niigata-shi, 950-2181 Japan.
†† The author is with Tsinghua University, 100084, P.R.China.
* Presently, with Mitsubishi Electric Corp.

their scattering matrices are described in Sect. 3. This result is confirmed by a laboratory measurement using a network analyzer. From the calculation and experimental results, we demonstrate that the formula of the compound scattering matrix is true for wire targets or point targets.

Although the wire-targets treated in this paper are primitive, it seems worth checking the result theoretically and phenomenologically. The result would provide a physical interpretation why real targets observed by a fully polarimetric SAR reveal as mixture of basic three scattering components. The wire-targets can be thought as a simplified model, for example, of tree branch or of vegetation within a resolution cell. The results obtained in this paper suggests that all the three components (sphere, diplane, and helix) can appear as a mixture even if the target is constructed by wires only.

2. Radar Polarimetry

2.1 Polarization State

If a single monochromatic, uniform, TEM plane wave propagates along the positive z direction, the complex instantaneous electric field in the transverse plane is expressed in the polarization basis (HV) as

$$\begin{aligned}\boldsymbol{E}_{(HV)} &= [E_H \boldsymbol{a}_H + E_V \boldsymbol{a}_V]\exp[j(\omega t - kz)] \\ &= [|E_H|\exp(j\phi_H)\boldsymbol{a}_H + |E_V|\exp(j\phi_V)\boldsymbol{a}_V] \\ &\quad \cdot \exp[j(\omega t - kz)] \\ &= [|E_H|\boldsymbol{a}_H + |E_V|\exp(j\phi)\boldsymbol{a}_V] \\ &\quad \cdot \exp[j(\omega t - kz + \phi_H)] \end{aligned} \tag{1}$$

where $\boldsymbol{a}_H$ and $\boldsymbol{a}_V$ are unit vectors in the H and V directions, respectively. $\phi = \phi_V - \phi_H$ is the phase difference between E_H and E_V. In general, the tip of the electric field as a function of time rotates an ellipse in a fixed transverse plane. Omitting the temporal term and the absolute phase, we can rewrite (1) as

$$\boldsymbol{E}_{(HV)} = |E_H|\boldsymbol{a}_H + |E_V|\exp(j\phi)\boldsymbol{a}_V \tag{1'}$$

Since the locus of the extremity of the electric field vector in a fixed transverse plane is an ellipse, it is convenient to employ the geometric parameters of the polarization ellipse (i.e., ellipticity angle ε, tilt angle τ, and size A) to represent the polarization wave as

$$\boldsymbol{E} = A \begin{bmatrix} \cos\tau & -\sin\tau \\ \sin\tau & \cos\tau \end{bmatrix} \begin{bmatrix} \cos\varepsilon \\ j\sin\varepsilon \end{bmatrix}. \tag{2}$$

The relationship between the two sets of notations is expressed as follows [2],

$$A^2 = |E_H|^2 + |E_V|^2 , \tag{3a}$$

$$\sin 2\varepsilon = \frac{2|E_H||E_V|\sin\phi}{|E_H|^2 + |E_V|^2} , \tag{3b}$$

$$\tan 2\tau = \frac{2|E_H||E_V|\cos\phi}{|E_H|^2 - |E_V|^2} . \tag{3c}$$

2.2 Scattering Matrix and Polarimetric Signature

In the (H-V) coordinate system, there exists a linear relation between the transmitted electric field and the scattered electric field. This relation is expressed as [2]

$$\boldsymbol{E}_s = [S]\,\boldsymbol{E}_i , \tag{4}$$

$$[S] = \begin{bmatrix} s_{HH} & s_{HV} \\ s_{VH} & s_{VV} \end{bmatrix}, \tag{5}$$

where $\boldsymbol{E}_i$ and $\boldsymbol{E}_s$ are the polarization states of the incident wave and the scattered wave, respectively. $[S]$ is a 2×2 complex element matrix, called the Sinclair scattering matrix. Since the absolute phase common to all elements is difficult to obtain in the measurement, relative scattering matrix is generally used to describe the scattering nature. In a reciprocal isotropic medium for the monostatic case, the reciprocity theorem holds and thus the Sinclair scattering matrix is symmetric, i.e.,

$$s_{HV} = s_{VH} . \tag{6}$$

In this case, the scattering matrices of five typical targets are listed as follows:

Sphere or Plate:

$$[S] = \begin{bmatrix} 1 & 0 \\ 0 & 1 \end{bmatrix};$$

Wire with an orientation angle ψ:

$$[S] = \begin{bmatrix} \cos^2\psi & \frac{1}{2}\sin 2\psi \\ \frac{1}{2}\sin 2\psi & \sin^2\psi \end{bmatrix};$$

Diplane [2] (the same meaning of dihedral corner reflector in this paper) with an orientation angle ψ:

$$[S] = \begin{bmatrix} \cos 2\psi & \sin 2\psi \\ \sin 2\psi & -\cos 2\psi \end{bmatrix};$$

Left helix with an orientation angle ψ:

$$[S] = \frac{1}{2}\exp(-j2\psi)\begin{bmatrix} 1 & j \\ j & -1 \end{bmatrix};$$

Right helix with an orientation angle ψ:

$$[S] = \frac{1}{2}\exp(j2\psi)\begin{bmatrix} 1 & -j \\ -j & -1 \end{bmatrix}.$$

Among these five simple targets, sphere (or plate) , diplane and left (and right) helix are the basical scattering targets. The scattering matrix of other targets can be described by

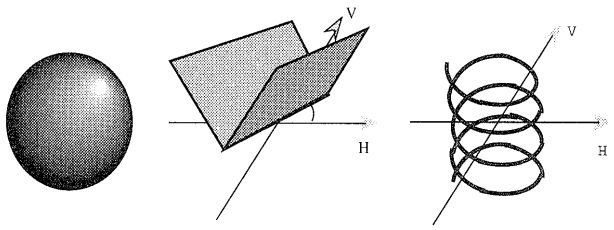

(a) Sphere (b) Diplane (c) Helix

Fig. 2 Shape of the three basic scattering targets.

sum of these three matrices. Shapes of these targets are shown in Fig. 2.

The received power of the backscattered signal, described by the combination of the scattering matrix and the polarization states for each antennas, is given by [3]

$$P = \left| \boldsymbol{E}_r^T [\, S \,] \boldsymbol{E}_t \right|^2 , \tag{7}$$

where $\boldsymbol{E}_t$ and $\boldsymbol{E}_r$ are the polarization states of the transmitted and the received wave, respectively. The superscript T denotes vector transpose. In the co-pol channel case where the polarization state of the receiver is identical with that of the transmitter, $\boldsymbol{E}_r$ is equal to $\boldsymbol{E}_t$. By using Eqs. (2) and (7) to express the received power, we can observe the polarimetric characteristics of the target visually and numerically by a polarimetric signature, which illustrates the polarimetric behavior of the target. A polarimetric signature is determined if a target scattering matrix is given. Figure 3 shows the polarimetric signatures of some typical targets, where gray scale is employed for indicating the value of the power with white for maximum and black for minimum. From a polarimetric signature, the characteristic polarization states can be obtained as the extreme values (max, null, saddle) of received power. For example, a wire whose orientation angle is 0 degree means that the wire is parallel to the H direction and is perpendicular to the V direction. In this case, the received power of horizontally polarized wave ($\varepsilon = 0, \tau = 0$) is maximum. Generally, the tilt angle τ of wire corresponds to the orientation angle, therefore the CO-POL Maxs of a wire target is $\tau = \psi$ (dependent on the orientation angle of the wire), and $\varepsilon = 0$ (linear polarization state).

2.3 Three Component Decomposition

Three Component Decomposition is a method to decompose a scattering matrix into three fundamental components: sphere, diplane and helix [2]. Mathematically, this method is expressed as

$$\begin{aligned} |\, S \,|_{HV} &= \left\{ e^{j\varphi_s} k_s |\, S \,|_{sphere} + k_d |\, S \,|_{diplane} + k_h |\, S \,|_{helix} \right\} \\ &\quad \cdot e^{j\varphi} \\ &= \left\{ e^{j\varphi_s} k_s \begin{vmatrix} 1 & 0 \\ 0 & 1 \end{vmatrix} + k_d \begin{vmatrix} \cos 2\psi_d & \sin 2\psi_d \\ \sin 2\psi_d & -\cos 2\psi_d \end{vmatrix} \right. \\ &\quad \left. + k_h \frac{1}{2} e^{\mp j 2\psi_h} \begin{vmatrix} 1 & \pm j \\ \pm j & -1 \end{vmatrix} \right\} e^{j\varphi} \end{aligned} \tag{8}$$

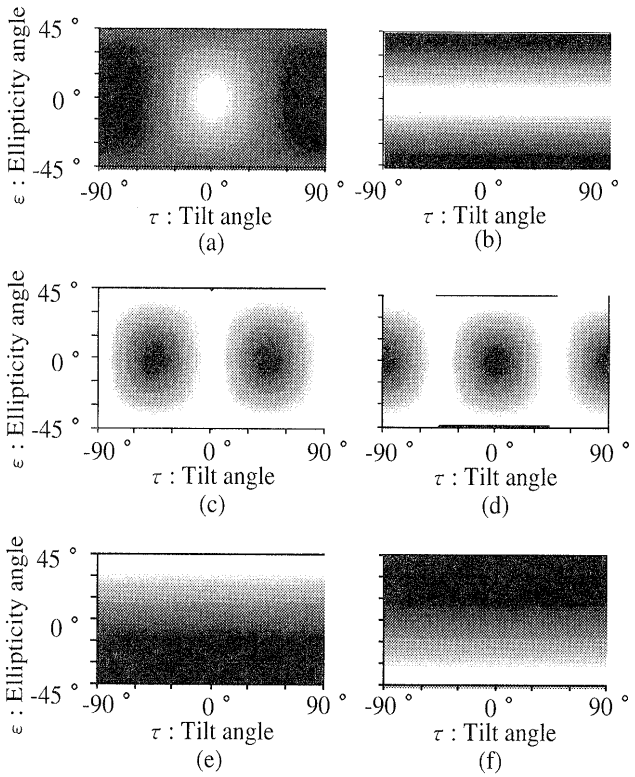

Fig. 3 Polarimetric signatures of typical targets in the co-pol channel case. (a) wire target ($\psi = 0°$); (b) plate and sphere; (c) diplane ($\psi = 0°$); (d) diplane ($\psi = 45°$); (e) right helix; (f) left helix.

where $[\, S \,]_{HV}$ denotes the scattering matrix in the HV polarization basis, and ψ_d and ψ_h are the orientation angle of the diplane and helix components, respectively. The phase components φ_s, φ containing the scattering center information of the components can be obtained uniquely when k_s, k_d and k_h are determined. For obtaining the coefficients of the three components: k_s, k_d and k_h, we first transform the target scattering matrix in the (H-V) basis into that in the circular (L-R) basis. Letting

$$[\, S \,]_{LR} = \begin{bmatrix} s_{LL} & s_{LR} \\ s_{RL} & s_{RR} \end{bmatrix} \tag{9}$$

denote the target scattering matrix in the circular basis (L-R), we have transformation

$$s_{RR} = \frac{1}{2} (s_{HH} - s_{VV}) + j\, s_{HV} , \tag{10a}$$

$$s_{LL} = \frac{1}{2} (s_{HH} - s_{VV}) - j\, s_{HV} , \tag{10b}$$

$$s_{LR} = s_{RL} = \frac{1}{2} (s_{HH} + s_{VV}) . \tag{10c}$$

Then the coefficients of the three components k_s, k_d and k_h are obtained as:

(i) for the case of $|s_{RR}| \geq |s_{LL}|$,

$$\begin{aligned} k_s &= |\, s_{LR} \,| , \\ k_d &= |\, s_{LL} \,| , \\ k_h &= |\, s_{RR} \,| - |\, s_{LL} \,| ; \end{aligned} \tag{11a}$$

Table1 Three components of typical targets.

	K_s	K_d	K_h
Sphere	1	0	0
Diplane	0	1	0
Wire	0.5	0.5	0
Right Helix Left	0	0	1

(ii) for the case of $|s_{RR}|<|s_{LL}|$,

$$k_s=|s_{LR}|,$$

$$k_d=|s_{LL}|,$$

$$k_h=|s_{LL}|-|s_{RR}|. \quad (11b)$$

From the above coefficients of the three components, it is possible to retrieve the sphere component, the diplane component and the helix component contained in a radar target. Table 1 shows the three components of the typical targets.

3. Compound Scattering Matrix

As shown in Fig. 1, if the radar range resolution is high enough ($d >> \Delta R$), the radar would discriminate two targets, and the corresponding scattering matrices would be $[S]_1$ and $[S]_2$, independently. However, if the radar range resolution is low ($d < \Delta R$), the radar cannot discriminate these two targets. Then what is the compound scattering matrix? The candidate formula may be

$$|S|_{total}=|S|_1+|S|_2\exp\left(-j\frac{4\pi d}{\lambda}\right) \quad (12)$$

where $[S]_1$ and $[S]_2$ denote the scattering matrices of the forefront target and the target behind, respectively. The spacing d contributes to the phase difference according to the propagation path. Note that no mutual coupling of targets is assumed in the above formula, because main purpose here is to show basic mechanism for mixture of multiple scattering. In reality, we cannot neglect mutual coupling when the targets are located closely, however, the basic concept can be confirmed by Eq. (12). We would like to verify Eq. (12) by using wires targets as a component of the mixture model that can be assumed as branches of tree or vegetations. In the following analysis and experiments, we assume that the wires are long with small radii compared to the wavelength.

Model 1
Suppose we have two wires which are oriented 45 and 135 degrees (Fig. 4), respectively. The corresponding scattering matrices are:

$$\psi_1=45^\circ \qquad [S]_1=\frac{1}{2}\begin{bmatrix}1&1\\1&1\end{bmatrix}, \quad (13a)$$

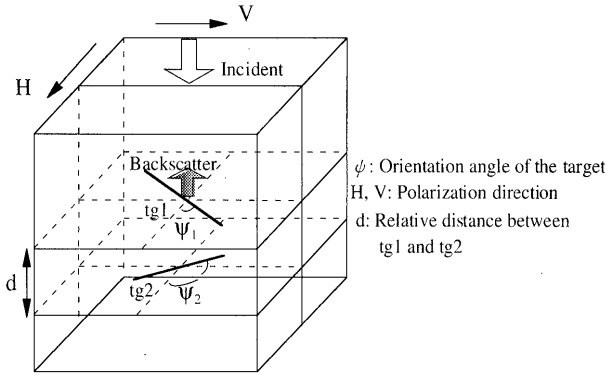

Fig. 4 Arrangement of two wire targets for Models 1 and 2.
Model 1: $\psi_1=45^\circ$, $\psi_2=135^\circ$
Model 2: $\psi_1=0^\circ$, $\psi_2=90^\circ$

$$\psi_2=135^\circ \qquad [S]_2=\frac{1}{2}\begin{bmatrix}1&-1\\-1&1\end{bmatrix}, \quad (13b)$$

where the angle ψ is the orientation of a wire with respect to the H direction. From Eq. (12), the compound scattering matrix depends on the distance d between the two wires.

(i) For $d=0, \frac{\lambda}{2}$, the corresponding phase difference is 0 or 2π, and therefore the compound scattering matrix is

$$[S]=\frac{1}{2}\begin{bmatrix}1&1\\1&1\end{bmatrix}+\frac{1}{2}\begin{bmatrix}1&-1\\-1&1\end{bmatrix}\exp(-j0)$$
$$=\begin{bmatrix}1&0\\0&1\end{bmatrix}. \quad (14a)$$

(ii) For $d=\frac{\lambda}{4}$, the corresponding phase difference is π, and the compound scattering matrix is

$$[S]=\frac{1}{2}\begin{bmatrix}1&1\\1&1\end{bmatrix}+\frac{1}{2}\begin{bmatrix}1&-1\\-1&1\end{bmatrix}\exp(-j\pi)$$
$$=\begin{bmatrix}0&1\\1&0\end{bmatrix}. \quad (14b)$$

The above results indicates that the composite wires with different spacing can become the generators of plate (or sphere), and diplane with 45 degree orientation angle.

Model 2
Suppose we use a horizontal wire and a vertical wire which have the following scattering matrices:

$$\psi_1=0^\circ \qquad [S]_1=\begin{bmatrix}1&0\\0&0\end{bmatrix}, \quad (15a)$$

$$\psi_2=90^\circ \qquad [S]_2=\begin{bmatrix}0&0\\0&1\end{bmatrix}. \quad (15b)$$

If we change the spacing d in Eq. (12), then the compound scattering matrix results in as follows:

(i) for $d=0, \frac{\lambda}{2}$ (the corresponding phase difference is 0 or 2π),

$$[S]=\begin{bmatrix}1&0\\0&0\end{bmatrix}+\begin{bmatrix}0&0\\0&1\end{bmatrix}\exp(-j0)$$
$$=\begin{bmatrix}1&0\\0&1\end{bmatrix}; \quad (16a)$$

(ii) for $d=\frac{\lambda}{4}$ (the corresponding phase difference is π),

$$[S]=\begin{bmatrix}1&0\\0&0\end{bmatrix}+\begin{bmatrix}0&0\\0&1\end{bmatrix}\exp(-j\pi)$$
$$=\begin{bmatrix}1&0\\0&-1\end{bmatrix}. \quad (16b)$$

The above results also indicates that the composite wires can become generators of plate (or sphere), and diplane.

Model 3.A

Now we use four wires which are oriented 0, 45, 90, 135 degrees, respectively. The corresponding scattering matrices are:

$$\psi_1=0^\circ \quad [S]_1=\begin{bmatrix}1&0\\0&0\end{bmatrix}, \quad (17a)$$

$$\psi_1=45^\circ \quad [S]_2=\frac{1}{2}\begin{bmatrix}1&1\\1&1\end{bmatrix}, \quad (17b)$$

$$\psi_3=90^\circ \quad [S]_3=\begin{bmatrix}0&0\\0&1\end{bmatrix}, \quad (17c)$$

$$\psi_2=135^\circ \quad [S]_4=\frac{1}{2}\begin{bmatrix}1&-1\\-1&1\end{bmatrix}. \quad (17d)$$

If the spacing d between two neighboring wires is $\frac{\lambda}{8}$ (shown in Fig. 5(a)), then the compound scattering matrix of the four wires is

$$[S]=\begin{vmatrix}1&0\\0&0\end{vmatrix}+\frac{1}{2}\begin{vmatrix}1&1\\1&1\end{vmatrix}\exp\left(-j\frac{\pi}{2}\right)$$
$$+\begin{vmatrix}0&0\\0&1\end{vmatrix}\exp(-j\pi)$$
$$+\frac{1}{2}\begin{vmatrix}1&-1\\-1&1\end{vmatrix}\exp\left(-j\frac{3\pi}{2}\right)$$
$$=\begin{vmatrix}1&-j\\-j&-1\end{vmatrix} \quad (18a)$$

This is identical with the scattering matrix of right helix.

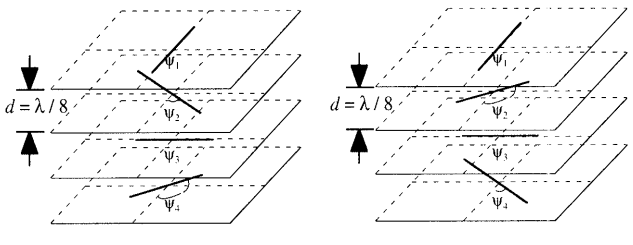

(a) (b)

Fig. 5 Arrangement of four wire targets for Model 3.
(a) $\psi_1=0^\circ, \psi_2=45^\circ, \psi_3=90^\circ, \psi_4=135^\circ$
(b) $\psi_1=0^\circ, \psi_2=135^\circ, \psi_3=90^\circ, \psi_4=45^\circ$

Model 3.B

Let us exchange the positions of the second and the forth wires, i.e., the orientation angles of the above four wires are 0, 135, 90, 45 degrees, respectively. Figure 5(b) shows the arrangement of the four wires. According to Eq. (12), we write the compound scattering matrix as:

$$[S]=\begin{vmatrix}1&0\\0&0\end{vmatrix}+\frac{1}{2}\begin{vmatrix}1&-1\\-1&1\end{vmatrix}\exp\left(-j\frac{\pi}{2}\right)$$
$$+\begin{vmatrix}0&0\\0&1\end{vmatrix}\exp(-j\pi)$$
$$+\frac{1}{2}\begin{vmatrix}1&1\\1&1\end{vmatrix}\exp\left(-j\frac{3\pi}{2}\right)$$
$$=\begin{vmatrix}1&j\\j&-1\end{vmatrix} \quad (18b)$$

This is identical with the scattering matrix of left helix. The Eqs. (18a) and (18b) demonstrate that four composite wires can become a generator of helix. This fact that multiple composite wires produce circularly polarized wave is important in the interpretation of polarimetric SAR image analysis because tree branches or vegetation leaves are similar to mixture of wire targets.

4. FDTD Analysis and Validation Experiment

4.1 FDTD Analysis

In order to check the applicability of the proposed formula, we carried out FDTD simulation [4], [5] on the compound scattering matrix for wires aligned in the range direction. The target scattering matrices are Eqs. (14a), (14b), (16a), (16b), (18a) and (18b). The reason why we used the FDTD method is its simplicity to simulate all the scattering phenomena including multiple reflections caused by wires correctly. The accuracy of the FDTD result used in this calculation is well adopted for the experimental verification accuracy.

Assuming that a linearly polarized plane wave with Gaussian pulse (3 GHz bandwidth) and its orthogonal polarization wave are incident on wires (Fig. 4) successively, then the corresponding scattered waves are calculated by the FDTD method. The range resolution in this case is 5 cm. Since the radar is located far from the wires, the scattered wave is calculated by far-field transformation based on the Green function formulation. Then the time domain signals are transformed to the frequency domain via FFT. The entire frequency characteristics of scattered field as well as the scattering matrix element at any frequency are thus derived.

Figure 6 and Fig. 7 show the polarimetric signatures derived from the FDTD calculation, corresponding to the model 1 and the model 2, respectively. The spacing d between the two wires varies from 0 to $\lambda/2$. From the inspection of these figures, it is understood that the polarimetric signatures depend on the spacing d. Furthermore, comparing Figs. 6 and 7 with Fig. 3, one

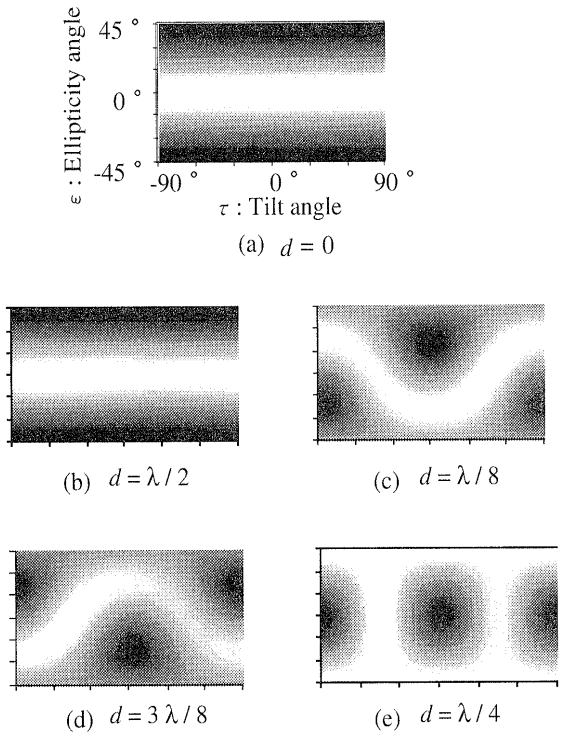

Fig. 6 Polarimetric signatures derived from FDTD method for Model 1.

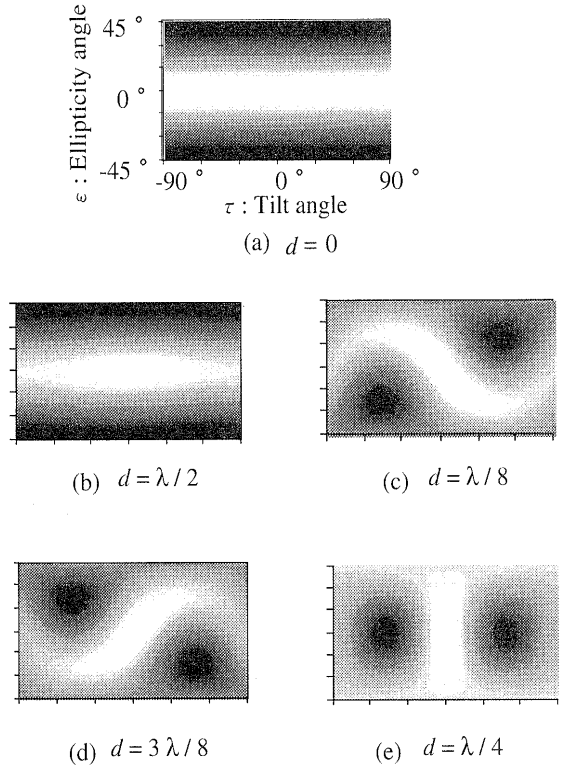

Fig. 7 Polarimetric signatures derived from FDTD method for Model 2.

observes that the signatures for $d = 0$ and $\lambda/2$ are similar to that of plate or sphere target, and that the signature for $\lambda/4$ resembles that of dihedral corner reflector, illustrating that the proposed formula of the compound scattering matrix is true for two wires.

In addition, the polarimetric signatures for model 3 are

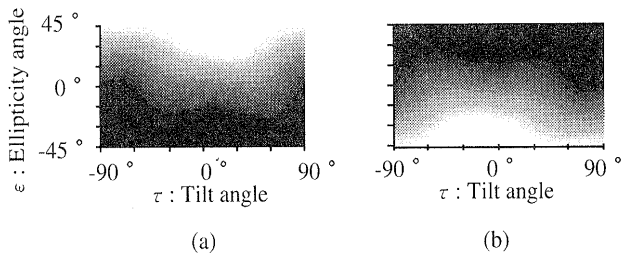

Fig. 8 Polarimetric signatures derived from FDTD method for Model 3. (a): Polarimetric signatures of Model 3.A, (b): Polarimetric signatures of Model 3.B.

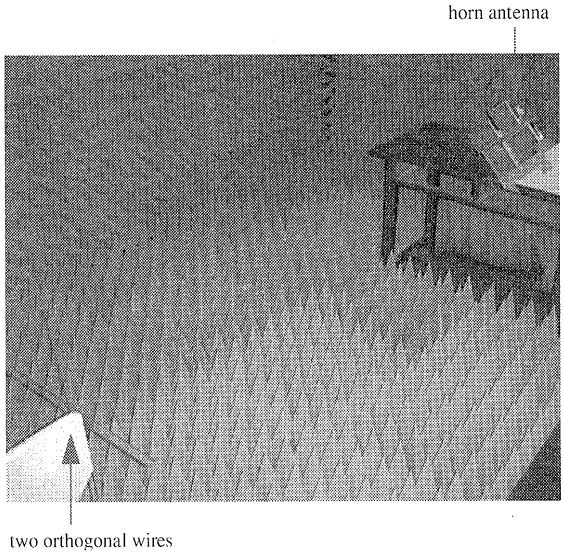

Fig. 9 Photograph of two wire targets and antennas for experiment in an anechoic chamber.

also shown in Fig. 7. Comparing Fig. 8(a) with Fig. 3(e) and Fig. 8(b) with Fig. 3(f), locations of the CO-POL MAX (white region) and CO-POL NULL (black region) almost coincide with each other, which also supporting the validity of the formula again.

Since the mutual coupling and reflected power imbalance of each wire are omitted in Eq. (12), one can observe slight difference between the polarimetric signatures in Fig. 8 and Fig. 3. However, the basic scattering characteristics are well understood and the validity is shown in the following experiment.

4.2 Validation Experiment

In order to confirm the proposed formula further, we carried out an experiment on the compound scattering matrix using a network analyzer (HP8720C). The experimental situation is illustrated in Figs. 9 and 10. In the experiment, the wire elements were selected to be 50 cm long with radius 3 mm. The experimental scattering matrix is evaluated at the frequency of 10 GHz. Figures 11 and 12 show the polarimetric signatures of the experimental results for the models 1 and 3, respectively. Comparing these figures with Figs. 6 and 8, one observes that the experimental result supports the hypothesis of Eq. (12).

For qualitative evaluation, we decomposed the

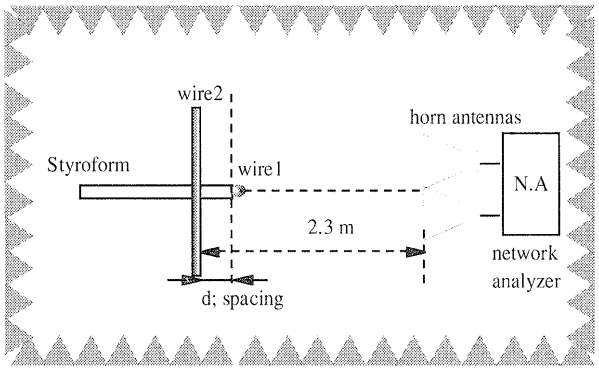

(a) Top view

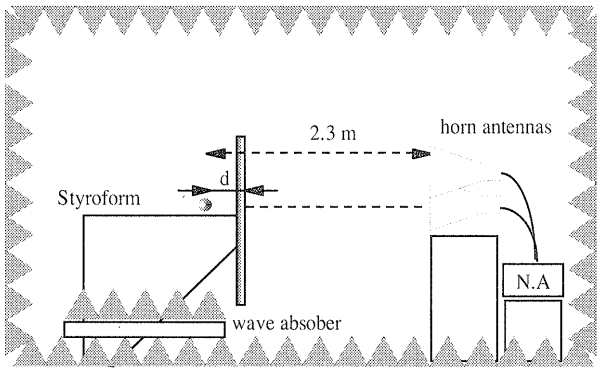

(b) Side view

Fig. 10 Imaging geometry used in the compound scattering matrix measurement of two wires.

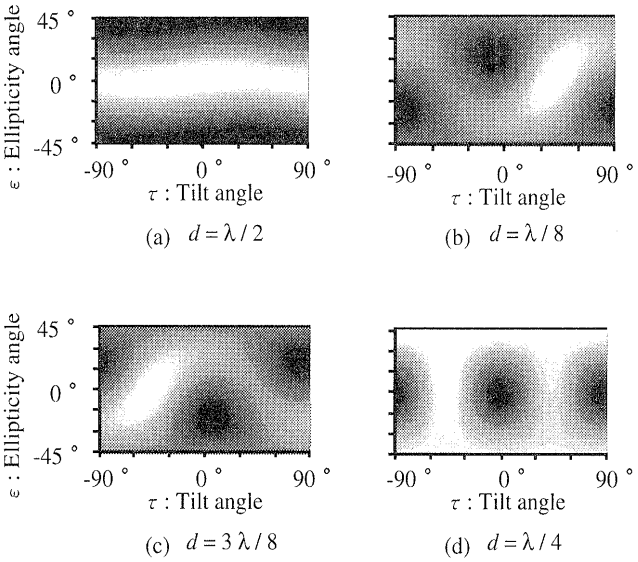

Fig. 11 Polarimetric signatures of experiment results for Model 1.

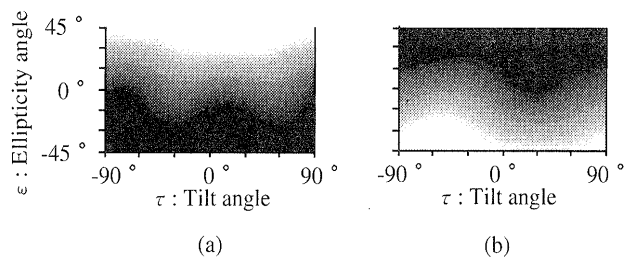

Fig. 12 Polarimetric signatures of experiment results for Model 3. (a) Polarimetric signatures for Model 3.A, (b) Polarimetric signatures for Model 3.B.

Table 2 Three decomposed components derived by FDTD method and experiment for Model 1.

distance d	FDTD			Experiment		
	plate	diplane	helix	plate	diplane	helix
$\frac{\lambda}{8}$	0.48	0.52	0	0.43	0.53	0.04
$\frac{\lambda}{4}$	0.05	0.95	0	0.04	0.91	0.05
$\frac{3}{8}\lambda$	0.51	0.49	0	0.46	0.52	0.02
$\frac{\lambda}{2}$	0.97	0.03	0	0.92	0.08	0.00

Table 3 Three decomposed components of experiment results for Model 3.

Model	Experiment		
	plate	diplane	helix
3.A	0.11	0.18	0.71
3.B	0.18	0.06	0.76

acquired scattering matrices into three fundamental components (i.e., plate, diplane, and helix components) by the Three Component Decomposition. Table 2 shows the results of decomposed ratio by the FDTD calculation and the experiment for the models 1 and 2. From the three decomposed ratio in this table, one can observe the validity of the proposed formula.

Table 3 shows the decomposed ratio of the experiment for the model 3. The helix ratio for the left and right helix-imitated wire target is greater than 0.7. There still exist sphere and diplane components. The main reasons are such that, 1) the mutual coupling is neglected in Eq. (12), 2) reflected power imbalance of each wire components are assumed to be the same, and 3) target alignment error affects the results. Although this helix ratio value is not unity, it is clear that the helix target can be realized by composite wires. This fact is very important in the interpretation of polarimetric SAR image of vegetation because there are so much similar situations.

5. Conclusion

The radar range resolution is determined by the frequency bandwidth of the transmitted signal. The wider the bandwidth, the finer the range resolution. If targets are aligned in the range direction, the compound scattering matrix is usually different from the scattering matrix of the forefront target. When the range resolution of a radar is smaller than a desired target length in the range direction, the scattering matrix becomes completely different from that of the forefront target and it represents a sum of neighboring elements in the range bin.

In this paper, wire targets aligned in the range direction were studied with respect to the compound scattering matrix. First, we proposed the formula of the compound scattering

matrix which consists of the scattering matrices of the single targets with the phase difference due to the spacing. For verifying this formula, we employed the FDTD method to analyze the scattering phenomena of wire targets aligned in the range direction. The calculation result demonstrated that two wires can become sphere and diplane component generators; and that four wires can become helix component generator. Finally, we verified this phenomenon with a laboratory measurement. From the results of the calculation and the experiment, one observes that the formula is true for wire targets. This result suggests that polarimetric analysis such as target decomposition should be carefully carried out. If the range resolution of a radar is not high enough, the scattering matrix of the desired target may be affected by the targets behind.

For complex shape target and large target with respect to range resolution, the polarimetric analysis will be examined in near future, since the FDTD scheme is easily extended to simulate complex shape target response.

Acknowledgement

This work in part was supported by Grant-in-Aid for Scientific Research, Ministry of Education, Japan.

References

[1] E. Krogager and Z.H. Czyz, "Properties of the sphere, diplane, helix decomposition," Proc. 3rd International Workshop on Radar Polarimetry, vol.1, pp.106-114, 1995.
[2] H. Mott, Antennas for radar communications—A polarimetric approach, John Wiley & Sons, New York, 1992.
[3] F.M. Henderson and A.J. Lewis, "Principle and applications of imaging radar," Manual of Remote Sensing, 3rd, ed. vol.2, Ch.5, John Wiley & Sons, 1998.
[4] K.S. Yee, "Numerical solution of initial boundary value problems involving Maxwell's equations in isotropic media," IEEE Trans. Antennas & Propag., vol.AP-14, pp.302-307, May 1966.
[5] A. Taflove, Computational electromagnetics the finite difference time-domain method, Artech House, Norwood, MA, 1995.
[6] K. Kitayama, Y. Yamaguchi, and H. Yamada, "Scattering matrix of line targets aligned in the range direction," Proc. 4th International Workshop on Radar Polarimetry, pp.96-105, July 1998.

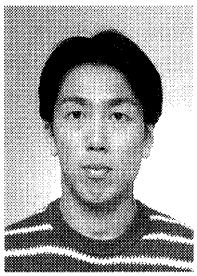

Kenji Kitayama was born in Toyama Prefecture, Japan, on September 16, 1974. He received the B.E. and M.E. degrees from Niigata University, Niigata, Japan, in 1997 and 1999, respectively. He was engaged in radar polarimetry and computer simulations. He is now with Mitsubishi Electric Corp., Information Technology R & D Center.

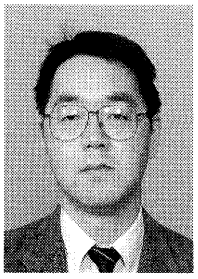

Yoshio Yamaguchi was born in Niigata, Japan, on March 12, 1954. He received the B.E. degree in electronics engineering from Niigata University in 1976, and the M.E. and Dr. Eng. degrees from Tokyo Institute Technology, Tokyo, Japan, in 1978 and 1983, respectively. In 1978, he joined the Faculty of Engineering, Niigata University, where he is a Professor. From 1988 to 1989, he was a Research Associate at the University of Illinois at Chicago. His interests are in the field of propagation characteristics of electromagnetic waves in lossy medium, radar polarimetry, microwave remote sensing and imaging. Dr. Yamaguchi is a senior member of IEEE, and a member of the Japan Society for Snow Engineering.

Jian Yang was born in Hubei Province, China, on February 1, 1965. He received the B.S. and M.S. degrees from Northwestern Polytechnical University, Xian, China, in 1985 and 1990, respectively, and Ph.D degree from Niigata University in 1999. He is now an Associate Professor at Tsinghua University, P.R. China. His interest includes radar polarimetry and its applications.

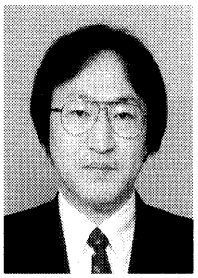

Hiroyoshi Yamada was born in Hokkaido, Japan, on November 2, 1965. He received the B.S., M.S., and Ph.D. degrees from Hokkaido University, Sapporo, Japan, in 1988, 1990, and 1993, respectively, all in electronic engineering. Since 1993, he has been with Niigata University, where he is an Associate Professor. His current research involves superresolution techniques, time-frequency analysis, electromagnetic wave measurements, and radar signal processing. Dr. Yamada is a member of IEEE.